MATHEMATICAL MODELING OF HEAT TREATING POWDER METALLURGY STEEL COMPONENTS

V. S. Warke, M. M. Makhlouf

A mathematical model to predict the response of powder metallurgy steels to heat treatment is presented and discussed. The model is based on modification of commercially available software that was originally developed for wrought alloys so that it can account for the effect of porosity. An extensive database had to be developed specifically for PM steels and includes porosity- and temperature-dependent phase transformation kinetics, and porosity- and temperature-dependent phase-specific mechanical, physical, and thermal properties. This extensive database has been developed for FL-4065 PM steel and has been used in the model to predict dimensional change, distortion, and type and quantity of metallurgical phases that develop in a typical PM component upon heat treatment. The model predictions are compared to measured values and are found to be in excellent agreement with them.

KEYWORDS: powder metallurgy, modelling, steel, heat treatment

INTRODUCTION

Components that are manufactured by the powder metallurgy process (PM) experience considerable changes during heat treatment. These include changes in their mechanical properties, dimensions, magnitude and sense of residual stresses, and metallurgical phase composition. Since most of the quality assurances criteria that these components have to meet include prescribed minimum mechanical properties and compliance with dimensional tolerances, it is necessary for producers of PM components to be able to accurately predict these changes in order to take appropriate measures to insure the production of parts that meet the required specifications. Several software packages that are capable of predicting the heat treatment response of wrought steels are available commercially [1-3], but none of them can predict the response of PM components. In this work, we developed a finite element-based model to predict the response of PM steels to heat treatment. The model is based on a modification of the commercially available software DANTE [3]. DANTE is comprised of a set of user-defined subroutines and can be linked to the finite element solver ABAQUS.

Virendra S. Warke, Makhlouf M. Makhlouf
Department of Mechanical Engineering - Worcester Polytechnic Institute - Worcester, MA 01609

Paper presented at the International Conference "Innovation in heat treatment for industrial competitiveness", organised by AIM, Verona, 7-9 May

The DANTE subroutines contain a mechanics module, a phase transformation module, and a diffusion module that are coupled to a stress/displacement solver, a thermal solver, and a mass diffusion solver, respectively. A block diagram showing the combined DANTE/ABAQUS model is shown in Fig. 1. The model requires an extensive database, which includes temperature- and porosity-dependent phase transformation kinetics, and temperature- and porosity-dependent phase-specific mechanical, physical, and thermal properties of the steel. We de-

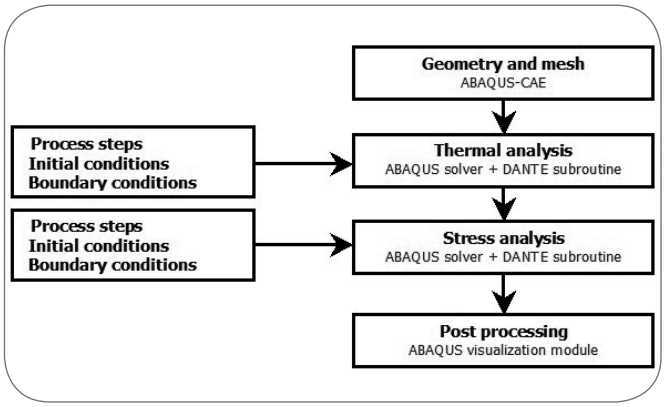

Fig. 1 ***Solution procedure for the DANTE/ABAQUS model.***
Procedura di soluzione per il modello DANTE/ABAQUS.

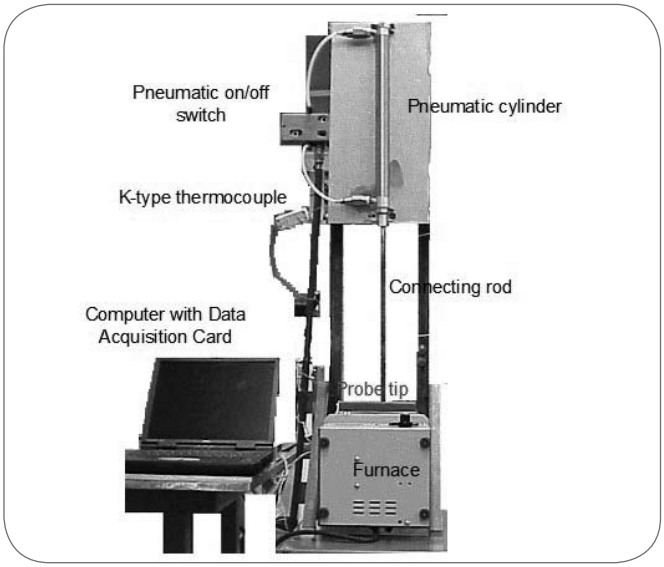

Fig. 2

Apparatus used to measure the heat transfer coefficient during quenching.

Dispositivo impiegato per la misurazione del coefficiente di trasferimento di calore durante la tempra.

veloped this database for FL-4065 PM steel and used it in the model in order to predict dimensional changes, distortion, and type and quantity of metallurgical phases that develop in the microstructure of a typical PM component upon heat treatment. In addition, we measured these characteristics for a commercially produced and heat treated part that was manufactured from FL-4065 PM steel and found the predictions of the model to be in excellent agreement with the measured values.

PROCEDURES AND MEASUREMENTS

Measurement of the Heat Transfer Coefficients

The method that we employed to measure the heat transfer coefficients during quenching involves quenching a heated cylindrical probe that is machined from the FL-4065 PM steel into the quenching medium and acquiring the temperature-time profile. The apparatus used for this purpose is shown in Fig. 2 and consists of an electric box furnace for heating the probe, a connecting rod that joins the probe to a pneumatic cylinder that allows automatic quenching of the probe into a beaker that contains the quenching oil, and a computer connected to a fast data acquisition system. A k-type thermocouple inserted at the geometrical center of the probe continuously measures the temperature of the probe. The probe dimensions are chosen such that the Biot number for the quenching process is < 0.1. This insures that significant thermal gradients will not be present in the radial direction of the probe. Hence, a simple heat balance analysis (usually referred to as a lumped parameter analysis) may be performed on the system (probe + quenching medium) to yield the heat transfer coefficient. With the Bi < 0.1, the error associated with such calculation of the heat transfer coefficient is less than 5%. A heat balance applied to the probe results in Equation 1, which is used to calculate the heat transfer coefficient at the surface of the probe.

$$(1) \quad h = -\frac{\rho V C_p}{A_s (T_s - T_f)} \frac{dT}{dt}$$

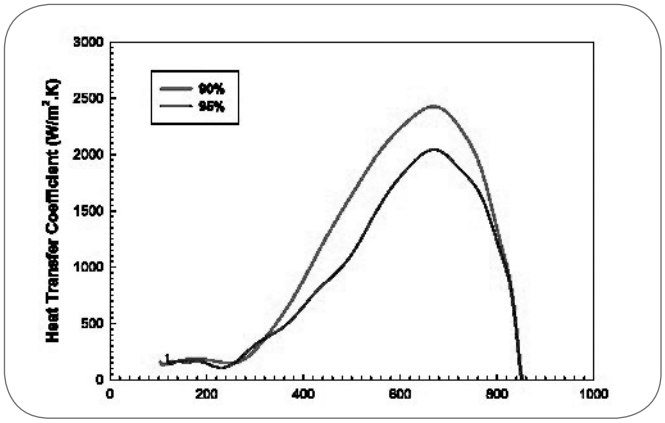

Fig. 3

Variation of the heat transfer coefficient with temperature and part density.

Variazione del coefficiente di trasferimento di calore in funzione di temperatura e densità del pezzo.

In Equation 1, h is the heat transfer coefficient at the surface of the probe, ρ, V, C_p, and As are the density, volume, specific heat, and surface area of the probe, respectively. T_s is the temperature at the surface of the probe, which due to the geometry of the probe is approximately equal to the measured temperature at the center of the probe, and T_f is the bulk temperature of the quenching medium. Fig. 3 shows the heat transfer coefficient obtained by this method for FL- 4605 PM steel probes processed to have different amounts of porosity.

Determination of the Phase Transformation Kinetics Parameters

We performed two types of dilatometric measurements on the samples in order to determine the kinetics of the phase transformations that occur during heat treatment [7]. These were (1) isothermal transformation measurements, and (2) continuous cooling transformation measurements. Data from the isothermal transformation measurements provided the kinetics parameters for the diffusive transformations, i.e., the austenite to bainite, and the austenite to ferrite/pearlite transformations, while data from the continuous cooling transformation measurements provided the transformation kinetics parameters for the austenite to martensite transformation. Fig. 4 shows the measured isothermal transformation curves for samples with 100% density undergoing the austenite to bainite transformation at different transformation temperatures. Fig. 5 shows the measured continuous cooling transformation curves for samples with 100% density transforming at different cooling rates.

We used the data generated from the isothermal and continuous cooling measurements to generate the kinetics parameters for the austenite to ferrite, austenite to pearlite, austenite to bainite, and austenite to martensite transformations and to create the Time-Temperature-Transformation-Porosity (TTTP) diagram for FL- 4605 PM steel, which is shown in Fig. 6.

Fig. 7 shows the data collected during tensile testing of 90% density austenite samples at three different temperatures. Similar curves were obtained for samples of each phase with 95% and 100% density as functions of temperature and strain rate. We used a fitting routine to fit this data to mathematical equations that we then used to create a mechanical property database.

It is important to note that, in addition to classical plasticity, i.e., the plastic flow caused by temperature cycling; the steel will ex-

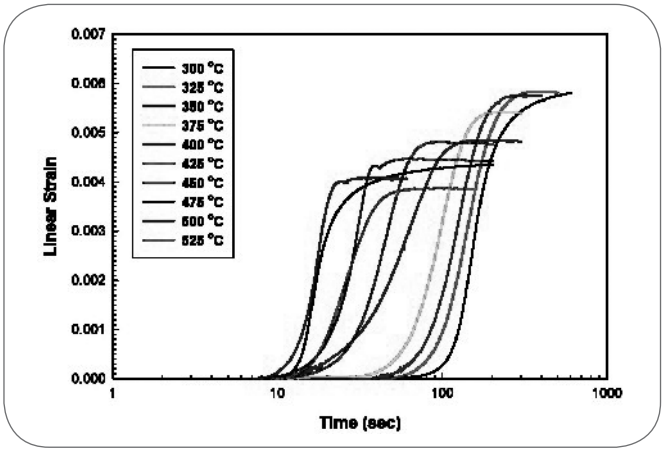

Fig. 4

Measured strain vs. time for the austenite to bainite transformation at different isothermal holding temperatures.

Misura della deformazione in funzione del tempo per la trasformazione da austenite a bainite durante trattamenti isotermi a temperature diverse.

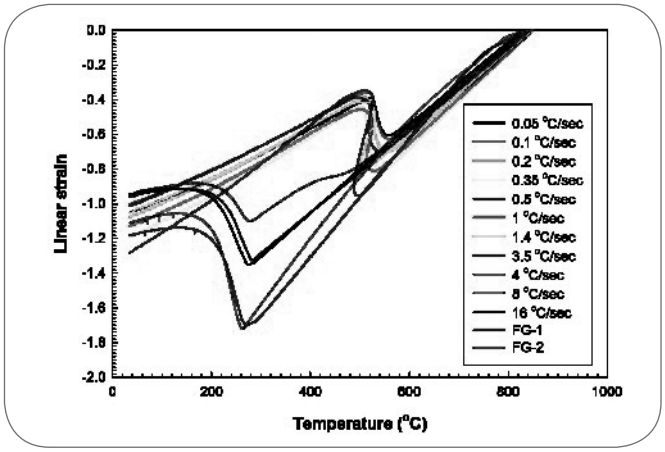

Fig. 5

Measured strain vs. temperature at different cooling rates during continuous cooling transformation measurements.

Misura della deformazione in funzione della temperatura per velocità di raffreddamento differenti durante le misure di trasformazione in raffreddamento continuo.

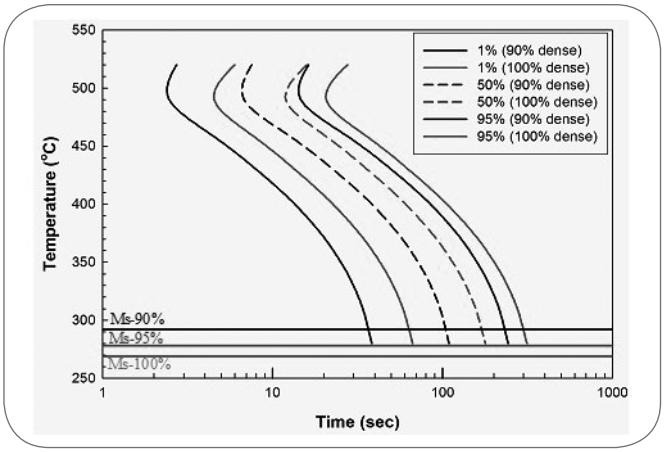

Fig. 6

TTTP diagram for 90% and 100% density FL-4605 PM steel plotted for the austenite to bainite and the austenite to martensite transformations.

Diagramma TTTP per densità 90% e 100% dell'acciaio FL- 4605 PM tracciato per le trasformazioni da austenite a bainite e da austenite a martensite.

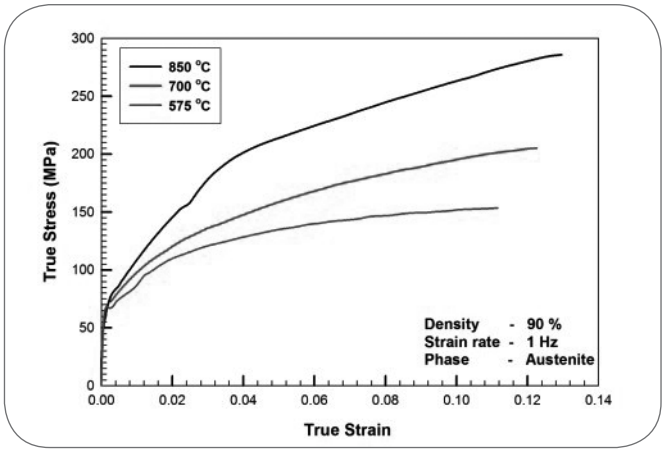

Fig. 7

True stress vs. true strain curve for austenite measured at three different temperatures for samples with 90% density at 1 s^{-1} strain rate.

Curva sollecitazione vs. deformazione per austenite, misurata a tre temperature diverse per campioni con densità 90% e velocità di deformazione 1 s^{-1}.

hibit transformation plasticity, i.e., plastic flow caused by change in the relative proportions of the various metallurgical phases in the microstructure brought about by the phase transformation. We used Low Stress Dilatometry in order to characterize this transformation-induced plasticity in FL-4605 PM steel. The procedure entails applying an external compressive static load to a standard specimen in a Gleeble machine just before the start of the transformation. We chose the magnitude of the applied load such that the magnitude of the resulting stress is less than the flow stress of austenite at the temperature of application of the load. We performed transformation induced plasticity measurements on samples of three densities (90%, 95%, and 100% of the theoretical density of the material) for each of the austenite to martensite and the austenite to bainite transformations. Fig. 8 (a) and Fig. 8(b) show the measured dilatation data for the 100% density sample at three the different applied stresses during the austenite to bainite and the austenite to martensite transformations, respectively. We performed similar measurements on samples with 90 % and 95% of theoretical density and used a fitting routine to fit this data to mathematical equations that were then used to create a transformation induced plasticity database.

MODEL CONSTRUCTION AND MATHEMATICAL SIMULATIONS

The capabilities of the model are demonstrated using the test part shown in Fig. 9. The dimensions of the part are summarized

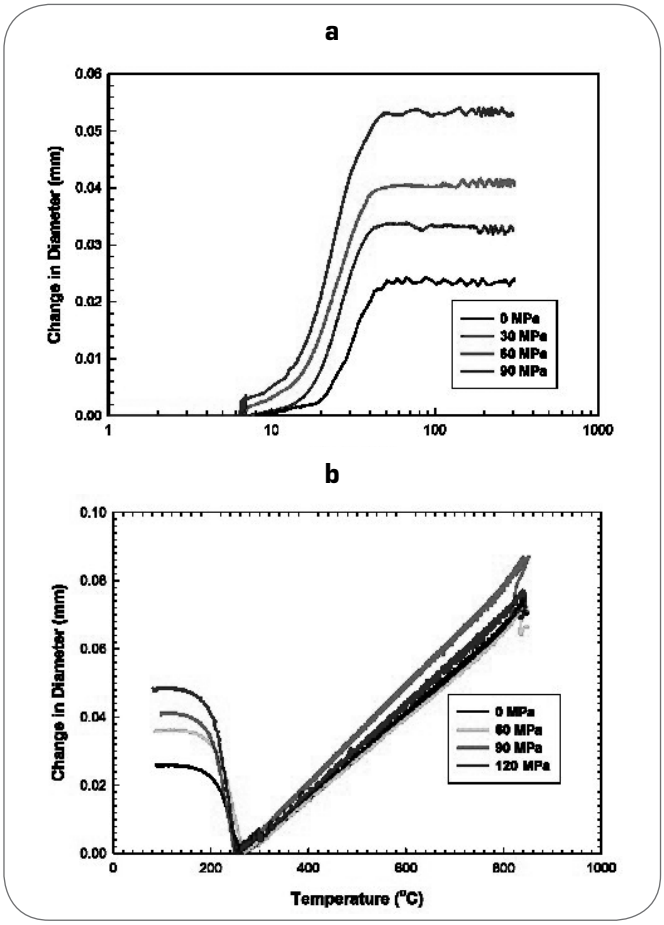

Fig. 8

Measured dilatation for samples with 100% density at three stress levels during (a) austenite to bainite transformation, and (b) austenite to martensite transformation.

Dilatazione misurata per i campioni con densità 100% a tre livelli di tensione durante (a) trasformazione da austenite a bainite, e (b) trasformazione da austenite a martensite.

in Tab. 1. Because of symmetry, only half of the part was modeled. Fig. 9 shows the 3-D part geometry created and meshed by the ABAQUS pre-processor. The meshed geometry contains 13,720 elements and 15,975 nodes. In order to capture the steep temperature gradient caused by quenching, the mesh was generated such that the density of nodes is higher near the surface of the part than in its interior.

Solution procedure and boundary conditions

The thermal module – We used the following sequence to model the heat treatment of the part: Furnace heating to 850°C, followed by immersion into the quench tank with a velocity of 40 mm/s, followed by quenching in oil to room temperature.

Dimension	Magnitude
Outer diameter	110.5 mm
Inner diameter	92.9 mm
Center offset	4.8 mm
Thickness	12.7 mm

Tab. 1

Dimensions of the test part.

Dimensioni delle parti in prova.

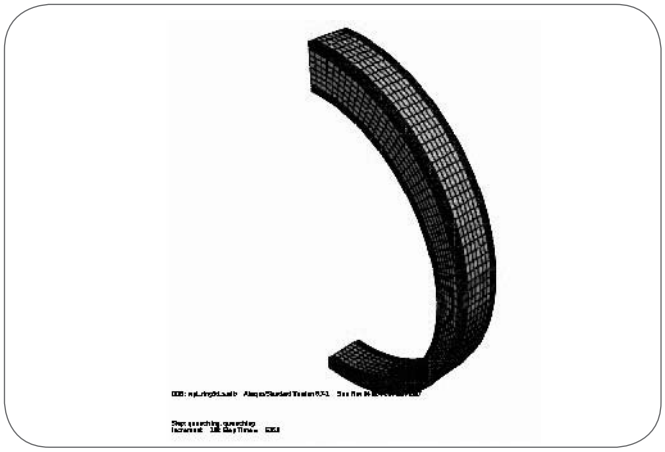

Fig. 9

Geometry and mesh used in the model.

Geometria e reticolo utilizzati nel modello.

The initial conditions that we used for the thermal module included the carbon content of the part, the temperature of the part before heat-treating (room temperature in this case), and the mode of heat treatment.

The boundary conditions that we used to represent each of the steps of the heat treatment process were as follows:

- For the furnace-heating step: We used a convective boundary condition at the surface of the part by providing the measured heat transfer coefficient for heating the part in the furnace up to the austenitizing temperature of 850°C.
- For the immersion step: We defined the direction and velocity of immersion of the part into the quench tank. This step is important in order to capture the temperature gradient along the immersion length of the part. In this demonstration, the part was immersed along its length with a velocity of 40 mm/s, and the process time for this step was 2.75 seconds.
- For the quenching step: We used a convective boundary condition at the surface of the part by providing the measured heat transfer coefficient for quenching the part in oil from the austenitizing temperature down to room temperature.

The stress module – This module uses mainly the time-temperature history of the part, which is generated by the thermal module, in order to calculate nodal displacements, stresses, and volume fraction of metallurgical phases.

For initial condition, we set the stress at all the nodes to zero. If a known initial stress state existed, we could have used the appropriate values. Nodal constraints are required in order to prevent rigid body displacement and rotation. This requirement applies to all the process steps, and is defined only once in the model input file. Referring to the 3-D geometry in Fig. 9, all the nodes of both symmetry faces were constrained from moving in the x direction. In addition, one node at the center of the top symmetry face was constrained from moving in the y and z directions, and one node at the center of the bottom symmetry face was constrained from moving in the z direction.

SIMULATION RESULTS AND COMPARISON TO MEASUREMENTS

In order to verify the accuracy of the model, we compared the model predictions to measurements that we performed on an

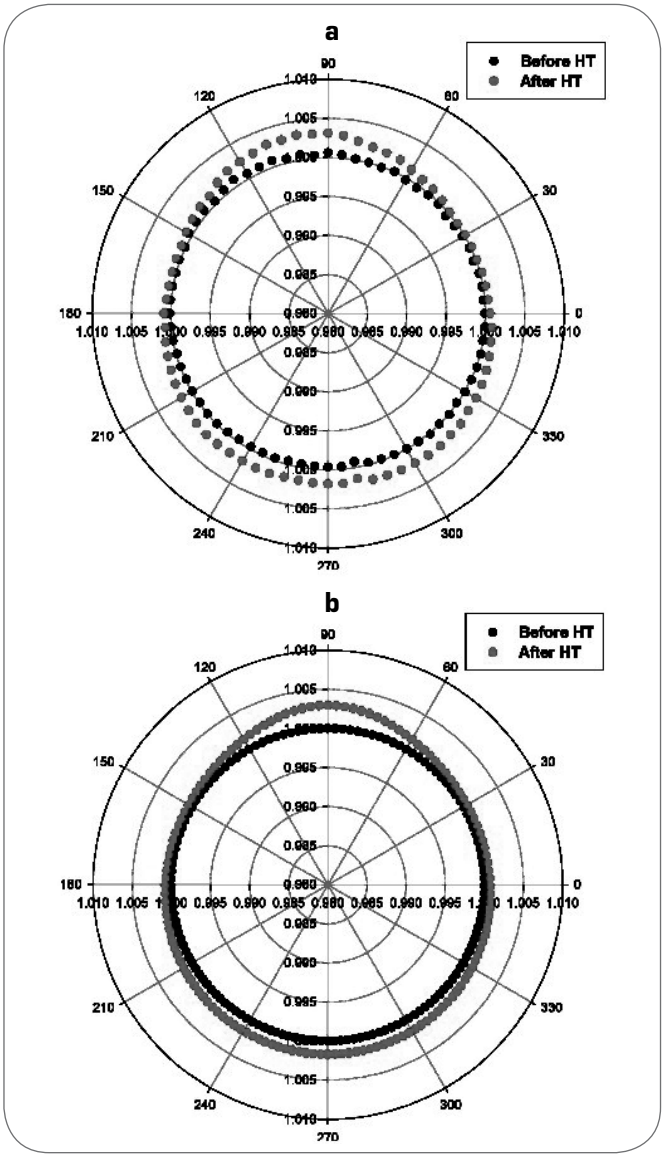

Fig. 10

Coordinates of the circular hole before and after heat treatment. (a) Measured using a CMM. (b) Predicted by the model.

Coordinate del foro circolare prima e dopo trattamento termico. (a) Misurato mediante CMM. (b) Previsione del modello.

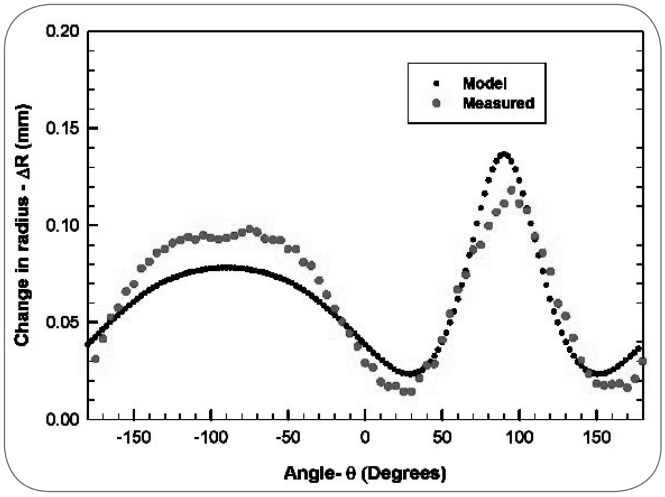

Fig. 11

Change in radius at different locations around the circular hole as predicted by the model and as measured by a CMM.

Variazione del raggio in diverse posizioni intorno ai fori circolari secondo la previsione del modello e misurato mediante CMM.

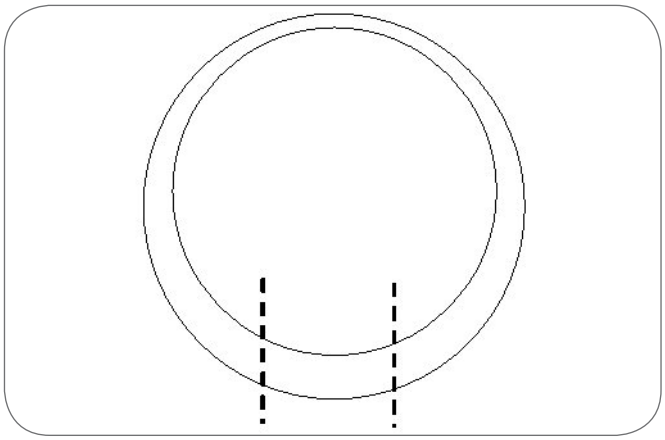

Fig. 12

Section lines showing where cuts were made for measuring retained austenite.

Linee di sezione che mostrano dove sono stati effettuati i tagli per misurare l'austenite residua.

FL-4605 PM steel component of configuration and dimensions similar to those used in the model.

Sample production – We admixed AUTOMET 4601 steel powder with Asbury 1651 graphite powder to yield 0.5 wt% carbon in the final product. We added zinc sterate to the powder as a lubricant, then placed the admixed powder in a die and pressed it using 216 tons of pressure. We sintered the green parts at 1100°C for 30 minutes in a continuous sintering furnace under a controlled atmosphere and then we air-cooled them to room temperature. The average measured density of the parts was 95% of theoretical density with negligible variation within each part and from part to part.

Heat treatment – The heat treatment cycle for the sintered parts consisted of furnace heating to 850°C, holding at this temperature for 20 minutes, and then quenching in oil with the parts placed in an upright position with their thinner section pointing down. Twenty parts were heat treated in an internal quench batch furnace under an endothermic atmosphere with 0.5 wt. % carbon.

In order to characterize the amount of distortion in the parts caused by the heat treatment we designed a fixture to hold the parts at the same location in a coordinate measurement machine (CMM). We measured the circular hole before and after heat treating the sample at locations around the periphery in 5° increments. We repeated the measurements at four depths along the thickness of the part and in each case we converted the xy measurement into a radius, r, and an angle θ at each measured point. We then normalized the radius by dividing it by the average radius before heat treatment. Fig. 10 and Fig. 11 compare the measured and model-predicted changes in dimensions of the central hole due to heat treatment.

In order to determine the fraction of metallurgical phases that formed during heat treatment we measured the amount of retained austenite in the heat treated parts using x-ray diffraction. We cut the parts along the dotted line shown in Fig. 12. We wet ground and polished the parts using standard metallographic techniques, and then we ultrasonically cleaned them. We performed the x-ray diffraction measurements according to ASTM E975 standard practice using a "θ- θ" type diffractometer . We performed the measurements at 3 different locations on each of 3 different parts using chromium Kα radiation. Fig. 13 shows a comparison of the model-predicted and the measured amount of retained austenite. It is clear that the model predictions are in excellent agreement with the measured values.

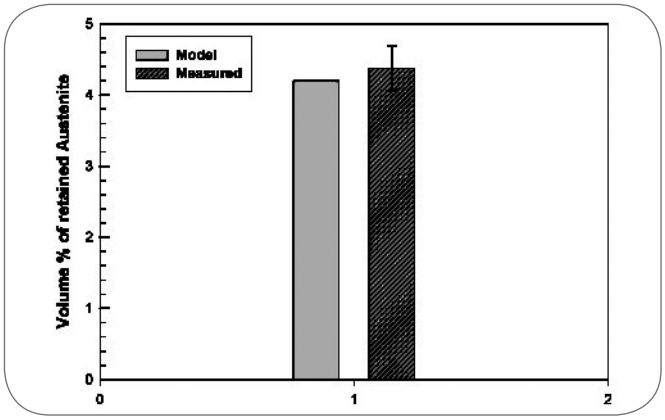

Fig. 13 ***Amount of retained austenite predicted by the model and measured by x-ray diffraction.***
Quantità di austenite residua secondo la previsione del modello e misurata mediante diffrazione ai raggi x.

SUMMARY

We modified the finite element based commercial software DANTE to enable it to predict the heat treatment response of powder metallurgy steels. We did that by introducing porosity as a state variable of the model.
We developed an extensive database for FL-4605 PM steel that contains information on phase transformation kinetics, elevated temperature mechanical properties, and heat transfer coefficients - all as functions of temperature and porosity for all possible phases, i.e., for austenite, ferrite, pearlite, bainite, and martenisite.
A side product of developing the database was creating, for the first time, a Temperature-Time-Transformation-Porosity (TTTP) diagram. Such diagrams are necessary for understanding and accounting for the effect of porosity that invariably exists in powder metallurgy components on the kinetics of phase transformations in PM steels.
Using the model, we simulated the heat treatment response of pressed and sintered powder metallurgy parts and we compared the model predictions to measurements made on heat treated parts that were commercially manufactured from FL-4605 PM steel. The dimensional changes and amount of retained austenite after heat treatment predicted by the model were found to be in excellent agreement with their measured counterparts.

ACKNOWLEDGEMENTS

The authors gratefully acknowledge the member companies of the Powder Metallurgy Research Center (PMRC) of Worcester Polytechnic Institute for their support of this work. In addition, the authors gratefully acknowledge the High Temperature Materials Laboratory User Program, Oak Ridge National Laboratory managed by UT-Battelle, LLC for the U.S. Department of Energy under contract number DE-AC05-00OR22725 for providing assistance with the dilatometric measurements.

REFERENCES

1] T. INOUE T. and K. ARIMOTO, Proc. Quenching and Distortion Control Conf., ASM Int, (1992) p.205.
2] N. JARVSTRAT and S. SJOSTROM, Proc. ABAQUS Users' Conf. (1993) p.273.
3] W. DOWLING, Proc. 2nd Int. Conf. on Quenching and Control of Distortion (1996) p.349.
4] M. MANIRUZZAMAN, Proc. 5th Int. Conf. on Frontiers of Design and Manufacturing (2002) p.619.
5] J.C. CHAVES, Ph.D. Dissertation (2001) Worcester Polytechnic Institute, Worcester, MA, p.133.
6] S. MA, Proc. 1st Int. Surface Engineering Congress, ASM Int. (2002) p.281.
7] ASTM Standard, A1033-04, "Recommended Practice for the Quantitative Measurement and Reporting of Hypo-Eutectoid Carbon and Low-Alloy Steel Phase Transformations".

ABSTRACT

MODELLAZIONE MATEMATICA DEL TRATTAMENTO TERMICO DI COMPONENTI IN ACCIAIO SINTERIZZATO

Parole chiave: metallurgia delle polveri, trattamenti termici, modellazione, acciaio

Nel lavoro si presenta e si discute un modello matematico per predire la risposta al trattamento termico degli acciai ottenuti da polveri metalliche. Il modello si basa sulla modifica del software disponibile in commercio, originariamente sviluppato per leghe da lavorazione, in modo tale che esso possa tenere in considerazione l'effetto della porosità. E' stata appositamente sviluppata un'ampia banca dati per l' acciaio sinterizzato FL-4065 comprendente informazioni su porosità e cinetica delle trasformazioni di fase dipendenti dalla temperatura, oltre ai rapporti tra porosità, fasi dipendenti dalla temperatura e proprietà meccaniche, fisiche e termiche. Questa vasta banca dati è stata utilizzata nel modello per prevedere cambiamenti dimensionali, distorsioni, il tipo e la quantità delle fasi metallurgiche che si originano in un tipico componente in acciaio sinterizzato durante il trattamento termico. Con lo sviluppo del database è stato creato, per la prima volta, un diagramma tempo-temperatura-trasformazione-porosità (TTTP). Tale diagramma si è rivelato necessario per comprendere e tener conto dell'effetto della inevitabile porosità che, nei componenti sinterizzati, rappresenta un fattore importante per la cinetica di trasformazioni di fase.
Mediante il modello, si è potuta simulare la risposta al trattamento termico di parti pressate e sinterizzate e si sono potute confrontare le previsioni basate sul modello con misurazioni effettuate su parti prodotte commercialmente con acciaio PM FL-4605, sottoposte a trattamento termico. La variazione dimensionale e la quantità di austenite residua dopo il trattamento termico previste dal modello si sono rivelate concordanti con i corrispondenti valori misurati.